JOURNAL OF CATALYSIS 143, 616–626 (1993)

Superacid and Catalytic Properties of Sulfated Zirconia

FANG REN CHEN,*,[1] GISÈLE COUDURIER,*,[2] JEAN-FRANÇOIS JOLY,† AND JACQUES C. VEDRINE*

*Institut de Recherches sur la Catalyse, CNRS, 2 Avenue Albert Einstein, F-69626 Villeurbanne Cédex, France; and †Institut Français du Pétrole, Laboratoire de Catalyse, 1-4 Avenue de Bois Préau F-92506 Rueil Malmaison Cédex, France

Received January 4, 1993; revised April 14, 1993

Zirconium hydroxide was sulfated by aqueous H_2SO_4 solutions of different normalities. The presence of sulfur was observed to slow down the decrease of the surface area and the tetragonal-to-monoclinic phase transformation of zirconia with increasing calcination temperature. Acidic properties were studied by the Hammett indicator technique. Charge transfer complex formation was studied by ESR using benzene as a probe to study strong ionizing properties of the samples, since benzene has a high ionizing potential value (9.24 eV). The observed ESR signal was assigned to biphenyl cation with hyperfine splittings equal to a_H = 6.74, 3.37, and 0.52 G for 2,4, and 4 protons, respectively. Its intensity was observed to be maximum for a calcination temperature equal to 600°C and a sulfur content equal to 1.5 to 3 wt%. This corresponds very probably to the maximum of strong Lewis acidity. Catalytic properties were studied for the isomerization of *n*-butane to i-butane in the 150 to 300°C range. The highest catalytic activity in flow reactor was observed for the samples calcined at 600°C as for benzene ionization properties, which indicates a close correlation. Hydrogen was observed to sharply decrease the deactivation rate suggesting that the active sites do not correspond to a sulfur-reduced species and that Brønsted acid sites are probably necessary for the reaction. It is proposed that both strong Lewis and Brønsted sites are involved for *n*-butane isomerization. Zr^{3+} cations were also observed by ESR for sulfated zirconia samples outgassed above 600°C with maximum intensity between 650 and 750°C. It is proposed that they arise from the reduction of Zr^{4+} cations by SO_4^{2-} decomposition into SO_2 and O_2. The presence of such Zr^{3+} species was not related to catalytic properties.

INTRODUCTION

Skeletal isomerization of normal paraffins is an important reaction in petroleum chemistry and is usually performed using liquid superacids or Pt on chlorinated alumina. However, it results in large environmental problems related to the recovery of aggressive and corrosive acids or to the necessary continuous supply of chlorinated compound to the reactants in course of the reaction. In order to overcome such problems, different solid superacids have been proposed, namely:

(i) combination of inorganic salts as $AlCl_3$–$CuSO_4$,

(ii) liquid superacid deposited on a suitable support,

(iii) sulfated sample or mixed metallic oxides as ZrO_2, Fe_2O_3, TiO_2, TiO_2–SiO_2, etc.,

(iv) metal-promoted superacid,

(v) superacid resins such as Nafion H or Amberlyst,

(vi) strongly acidic zeolites such as dealuminated mordenite or more or less aluminated H–MFI zeolites.

Recent review papers have been published on this subject (*1–7*), particularly on sulfated oxides thought to replace the Pt/chlorinated alumina catalyst (*8*). Superacidity which was first mentioned by Conant and Hall in 1927 at the American Chemical Society, was studied by Olah (*9*) in his works

[1] Present address: Department of Chemistry, University of Wisconsin, P.O. Box 413, Milwaukee, WI 53201.

[2] To whom correspondence should be addressed.

0021-9517/93 $5.00

on carbonium ions in the 1960s and by Gillespie in 1968 (*10*). From the latter work, the definition of superacid was arbitrarily settled for Hammett's function H_0 such as $H_0 < -11.9$ which corresponds to pure sulfuric acid. For characterizing such acidity, several techniques were developed, namely, physicochemical techniques, test reactions, or theoretical calculations. However, none of them were really satisfactory, for solids in contrast to liquids. As a matter of fact, the concept of pH has no meaning for solids and comparison with liquid properties is usually necessary.

ESR is known to be able to detect paramagnetic carbocations formed by charge transfer between surface sites and organic molecules. With organic molecules difficult to ionize, the technique allows one to detect strong ionizing sites. For instance, we have shown previously (*13*, *14*) that benzene (ionization potential equal to 9.24 eV) could only be ionized by strong acid sites as in H–ZSM-5 or H–mordenite zeolites and not by less acidic zeolites as in H–Y. In the former case, the $C_6H_6^+$ cation may even dimerize in sandwich-like $(C_6H_6)_2^+$ dimers, if there were a void volume large enough, as in H–mordenite with respect to H–ZSM-5.

In the present work acidity characterization was carried out mainly using ESR in comparison with catalytic data. Studies using IR were published recently (*11*), while a conjoint IR-theoretical study will be published shortly (*12*).

EXPERIMENTAL

Sample Preparation

Zirconium hydroxide was prepared as follows: 64.4 g of $ZrOCl_2 \cdot 8H_2O$ were dissolved in 500 cm^3 of water (0.5 *M*) at room temperature; 28 wt% aqueous NH_4OH solution was added dropwise under vigorous stirring at room temperature up to a pH of 8.4. The gel was then filtered and washed with permuted water until there were no detectable chlorine ions in the washing water. The gel was dried at 120°C for 24 h. The dry gel was introduced into an H_2SO_4 solution of normality *N* for 20 min at room temperature and then filtered without washing, dried at 120°C for 24 h, and calcined under static air conditions or under air flow at the desired temperature (400 up to 800°C) with a heating rate of 4°C min^{-1} for 3 h. Samples are designated SO_4^{2-}/ZrO_2-*N*, in the following.

Acidity Characterization

For Hammett's indicator technique, 2.4 dinitro fluorobenzene with $H_0 = -14.52$ was placed into a small ampoule and evacuated by a freeze–pump–thaw procedure. After the samples were outgassed at 500°C for 1 h, they were cooled down to room temperature and then contacted with the above indicator by breaking the ampoule *in situ*.

The ESR analysis was carried out with a Varian E9 spectrometer at room temperature in the X band. The samples were placed in an ESR silica tube (4 mm i.d.), outgassed at a desired temperature for 1 to 5 h. Benzene at its vapor pressure at room temperature was contacted at room temperature with the sample. Benzene was deoxygenated previously by the freeze–pump–thaw technique. Quantitative data were estimated by integrating the derivative curves and comparing the surface of the integrated peak with that taken under the same conditions with the Varian strong pitch (3×10^{15} spins/cm length).

Other Characterizations

Catalytic properties were studied for *n*-butane isomerization using a differential microreactor and gas chromatographic detection on line. The flow rate was 2 dm^3 h^{-1} with 200 mg catalyst, $P_{butane} = 9 \times 10^3$ Pa, and N_2 as carrier gas.

XPS analysis was carried out in vacuo with an HP5902 spectrometer for the different samples as such, i.e., without any treatment in the apparatus.

X-ray diffraction studies were performed with a Siemens K710 X-ray source equipped

TABLE 1

Sulfur Content from Chemical Analysis and Surface Area for Samples Calcined at 500°C under Air Flow

Samples	S content (wt%)	Surface area ($m^2\ g^{-1}$)
$Zr(OH)_4$	0	288[a]
ZrO_2	0	54[a]
SO_4^{2-}/ZrO_2-0.04 *N*	1.0	108
SO_4^{2-}/ZrO_2-0.08 *N*	1.9	107
SO_4^{2-}/ZrO_2-0.2 *N*	2.2	111
SO_4^{2-}/ZrO_2-0.28 *N*	2.6	113
SO_4^{2-}/ZrO_2-0.4 *N*	3.1	106
SO_4^{2-}/ZrO_2-1 *N*	4.1	115
SO_4^{2-}/ZrO_2-3 *N*	7.2	26
$Zr(SO_4)_2 \cdot 8H_2O$	15.0	4.6[a]

[a] 200°C calcination for 1 h.

with a Cu anticathode and a Phillips PW 1710 goniometer.

BET surface area measurements were carried out at liquid-nitrogen temperature in an automated laboratory made equipment.

Chemical analysis of sulfur content was performed at the Central Analysis Service Laboratory of CNRS in Solaize, France.

RESULTS AND DISCUSSION

The sulfur content and surface area values are reported in Table 1 for all the samples calcined under air flow at 500°C. An increase of the sulfur content is observed as a function of the normality of the H_2SO_4 solutions.

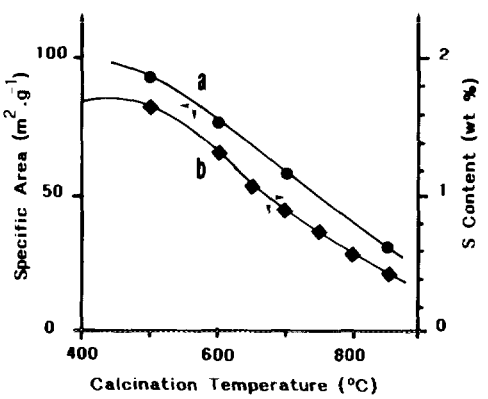

FIG. 1. Variations versus calcination under static atmosphere of (a) surface area and (b) sulfur content for the SO_4^{2-}/ZrO_2-0.08 *N* sample.

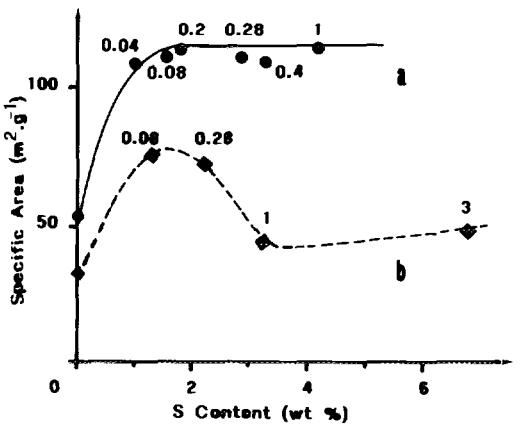

FIG. 2. Variations of surface area versus S content and calcination temperature: (a) 500°C and (b) 600°C. Numbers on the curves indicate the impregnation solution normality.

SO_4^{2-}/ZrO_2-0.08 *N* sample was studied in more detail than the other samples. The variations of its sulfur content and surface area values as a function of the calcination temperature under static conditions are reported in Fig. 1. It clearly appears that calcination resulted in a departure of S particularly above 600°C and that the surface area decreased in a parallel way.

In Fig. 2, the surface area values are plotted as a function of the sulfur content, for a same calcination temperature (500 or 600°C) and for all the samples. It appears that after calcination at 500°C, all the sulfated samples had the same surface area (≈110 $m^2\ g^{-1}$) whatever the sulfur content was. Comparison with nonsulfated ZrO_2 (54 $m^2\ g^{-1}$) led to conclude that the presence of sulfur stabilized high surface area, as observed for many other cations or anions (*15*). For samples calcined at 600°C, the surface area had a maximum value for a sulfur content around 2% and then decreased although remaining higher (≈45 $m^2\ g^{-1}$) than for pure ZrO_2 (34 $m^2\ g^{-1}$).

XRD studies showed that all the samples were amorphous below 400°C, crystallized as tetragonal ZrO_2 phase between 400 and 600°C, and changed into monoclinic ZrO_2 phase above 700°C. In the same conditions, pure ZrO_2 was monoclinic.

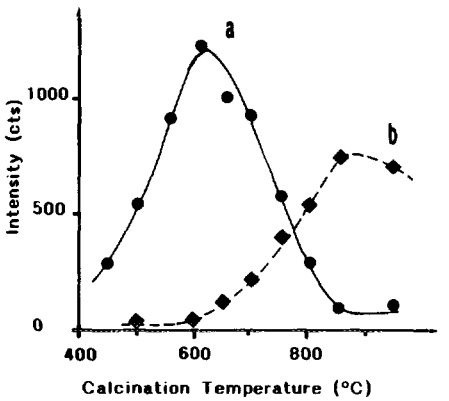

FIG. 3. XRD peak intensity variations versus calcination temperature under static air atmosphere for SO_4^{2-}/ZrO_2-0.08 *N*: (a) tetragonal ZrO_2 phase (2Θ = 30.240) and (b) monoclinic ZrO_2 phase (2Θ = 28.150).

The XRD intensities of the peaks at $2\Theta = 30.240°$ (characteristic of tetragonal ZrO_2) and at $2\Theta = 28.150°$ (characteristic of monoclinic ZrO_2) are reported in Fig. 3 as a function of the calcination temperature for the SO_4^{2-}/ZrO_2-0.08 *N* sample. It is observed that the tetragonal phase was mainly present at 600°C.

Comparison of the various samples calcined at 600°C shows that a maximum of crystallinity was obtained for sulfur contents around 1–2%.

2,4 Dinitrofluorobenzene ($H_0 = -14.52$) was used as a Hammett indicator. Its color should change from light yellow to orange when acidity moves from strong acid to superacidic media.

However, the choice of a suitable solvent for the method of the Hammett indicators was unsuccessful because the solid samples were immediately colored in many solvents such as benzene or hexane, as it has already been observed (*16*). Thus, gaseous 2,4-dinitrofluorobenzene has to be used. It was adsorbed in our case on the outgassed samples at its partial pressure at room temperature.

The yellow-orange color of the conjugate acid form was observed for all the sulfated samples and also, although to a smaller extent, for the nonsulfated ZrO_2. A similar observation was mentioned by Mukaida *et al.* (*17*), who showed that ZrO_2 is already in the superacid region beyond the border $H_0 = 11.93$ using the Hammett indicator technique.

As ZrO_2 was inactive for *n*-butane isomerization while sulfated zirconia was active, one can conclude that the Hammett indicator technique using gaseous 2,4-dinitrofluorobenzene is not appropriate for our purpose.

ESR turned out to be valuable for our purpose. When pure zirconia was outgassed at 400 or 500°C, no ESR spectrum was detected unless a weak signal near $g = 2.003$. At variance, sulfated zirconia samples exhibited an axial-type spectrum with $g_\perp = 1.979$ and $g_\parallel = 1.951$ (Fig. 4) when outgassed above 600°C, which corresponds to a d^1 ion, very probably Zr^{3+} as observed by Morterra *et al.* (*18*). Referred to the Varian strong pitch (3×10^{15} species per cm height of sample in the ESR tube), the number of Zr^{3+} ions can be estimated to 15×10^{14} ions per g for the 650°C outgassed sample. When oxygen was further introduced at increasing

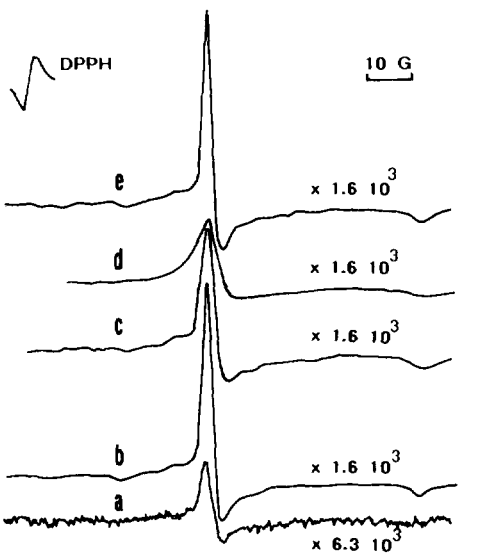

FIG. 4. Room temperature ESR spectrum of ZrO_2 samples: (a) pure ZrO_2 reduced 1 h under H_2 at 500°C, (b) SO_4^{2-}/ZrO_2-1 *N* sample outgassed at 650°C for 1.5 h, (c) b + O_2 (7.10^2 Pa) 5 min, (d) c + O_2 (28.10^2 Pa) 20 min, and (e) d outgassed at room temperature 30 min.

pressure, no signal of O_2^- was detected but the ESR signal of Zr^{3+} was broadened (Figs. 4b and 4c). This is typically due to the well known effect of loosely bound oxygen which is paramagnetic. This broadening was reversible since the signal completely recovered upon removing oxygen by outgassing (Fig. 4e). This result indicates that the Zr^{3+} species are located at the surface of the zirconia crystallites. The signal intensity varied with outgassing temperature as shown in Fig. 5. This intensity is expressed in arbitrary units per surface area, since as shown above the Zr^{3+} species are superficial. These Zr^{3+} species clearly appeared only for the sulfated zirconia and were formed mainly for outgassing temperatures above 600°C. As it has been observed that this range of temperature corresponds to the decomposition of the sulfated species, one may suggest the following reaction:

$$2Zr^{4+} + SO_4^{2-} \rightarrow 2Zr^{3+} + SO_2 + O_2.$$

The formation of SO_2 by sulfate decomposition has indeed been detected for sulfated ferric oxide (*19*).

When benzene was adsorbed on pure zirconia as described in the Experimental section no ESR spectrum was observed whatever the calcination temperature was, even in the presence of oxygen known to greatly enhance charge transfer complex intensity (*19*). On the contrary, for sulfated samples

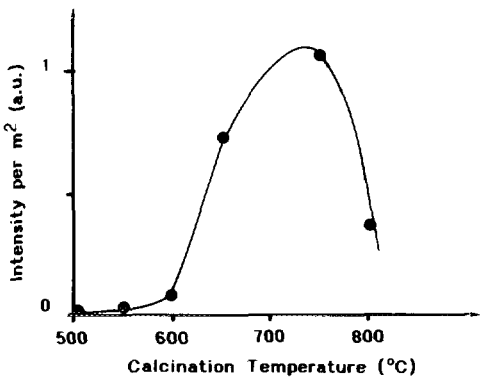

FIG. 5. Variations of the Zr^{3+} ESR signal intensity as a function of outgassing temperature for the SO_4^{2-}/ZrO_2-1 *N* sample.

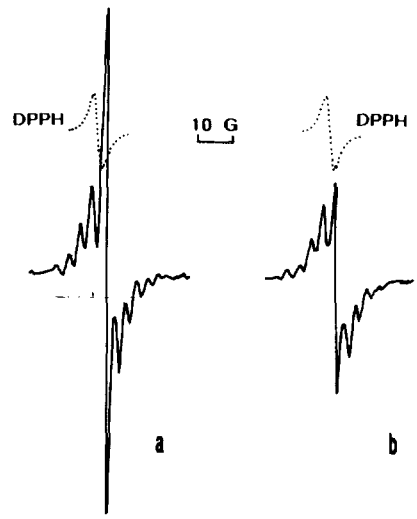

FIG. 6. ESR spectra of paramagnetic species as recorded after contacting the SO_4^{2-}/ZrO_2-0.08 *N* sample with benzene at room temperature under its partial pressure at the same temperature (a) after 1 min and (b) after 5 min.

a new ESR spectrum with nine hyperfine lines was obtained for samples outgassed at different temperatures with a slight decrease, if any, of the Zr^{3+} ion signal. The new signal centered at g = 2.0022 was composed of a nine-hyperfine-line spectrum and a superimposed narrow peak at $g = 2.0022$ ($\triangle H_{pp} \approx 1.5$ G) (Fig. 6). The narrow peak intensity decreased rapidly with contacting time of benzene while the nine-hyperfine-line spectrum decreased slowly, as shown in Fig. 7. The latter signal had a hyperfine splitting equal to 3.3 G.

The $C_6H_6^+$ and sandwich-like $(C_6H_6)_2^+$ radical cations are known (*13*, *14*) to give a hyperfine splitting equal to 4.4 and 2.2 G with 7 and 13 hyperfine lines, respectively. The hyperfine splitting as observed (3.3 G) and the number of hyperfine lines (=9) led us to suggest that the radical is different and indeed corresponds to a biphenyl cation. As a matter of fact such, a radical cation (*20*, *21*) was shown to have the following couplings: $a_H = 3.37$ G for protons 2, 6, 8, and 12; 6.74 G for terminal protons 4 and 10; and 0.52 G for protons 3, 5, 9, and 11 against 2.73, 5.46, and 0.43 G for the anion (*22*).

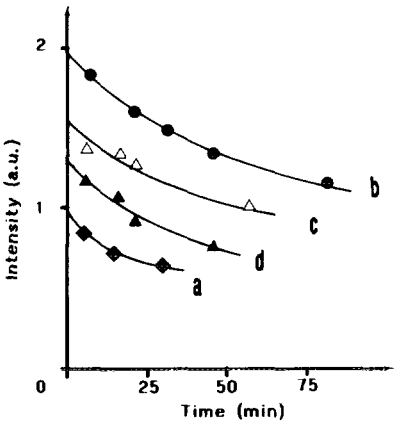

FIG. 7. Variations of the nine-hyperfine-line spectrum due to biphenyl cation versus time at room temperature for the following samples: (a) SO_4^{2-}/ZrO_2-0.4 *N*, 500°C; (b) SO_4^{2-}/ZrO_2-0.4 *N*, 600°C; (c) SO_4^{2-}/ZrO_2-0.4 *N*, 660°C; (d) SO_4^{2-}/ZrO_2-0.28 *N*, 500°C. The temperature is the outgassing temperature before cooling to room temperature and introducing benzene.

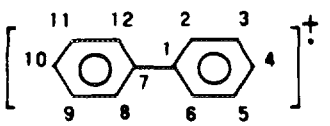

This gives a nine-hyperfine line-spectrum since one splitting for two protons (4 and 10) (giving $2nI + 1 = 3$ lines of 1 : 2 : 1 relative intensities) is double that for four other protons (2, 6, 8, and 12) (giving $2nI + 1 = 5$ lines of 1 : 4 : 6 : 4 : 1 relative intensities) and the third one is relatively negligeable (≈0.5 G). The hyperfine structure is described by a bar representation in Fig. 8. The 3.37 G splitting is close to the 3.3 G splitting observed in our case. This biphenyl cation was suggested (*20, 21*) to arise from a reaction of benzene cation $C_6H_6^+$ (a_H = 4.4 G) with neutral benzene molecule according to:

The narrow central line ($\triangle H_{pp} \approx 1.5$ G) was observed to decrease rapidly in intensity with time and presumably corresponds to a free electron. Free radicals such as charge transfer complexes are known to be instable and to decompose or react between themselves with time.

The biphenyl cation signal intensity was followed as a function of time at room temperature after contacting benzene vapor. It decreased slowly with time (Fig. 7) certainly because the biphenyl cation is bulkier than the free electron species. Its decrease was similar for all samples and one can thus reasonably take the intensity value after 5 min for all samples for comparison.

The variations of intensity of the hyperfine spectrum (assigned to biphenyl cation) as a function of outgassing temperature and sulfur content are shown in Fig. 9. It clearly appears that the highest intensity was obtained for outgassing at 600°C and with sulfur content in a range of 1.5 to 3 wt% with an intensity value of roughly 6×10^{15} spins g^{-1}, i.e., of the order of 10^{-2} μmol g^{-1}, assuming that such a quantification has a meaning in ESR.

When the samples were further contacted with oxygen (≈1 kPa) or with air at room temperature, the color turned from white to grey while the nine-hyperfine-line spectrum disappeared immediately and a huge signal appeared (Fig. 10). This signal of an intensity roughly 100 times higher than that of the biphenyl cation is typical of a carbonaceous residue with $g = 2.0021$ and $\triangle H_{pp} = 6.7$ G, ionized by oxygen. As no hyperfine structure was observed, the species could not be identified more precisely. In addition, a sublying spectrum with $g_{zz} = 2.027$, $g_{yy} = 2.010$, and $g_{xx} = 2.002$ of lower intensity was appearing. This signal is typical of O_2^- species (*23–25*), with the g_{zz} value

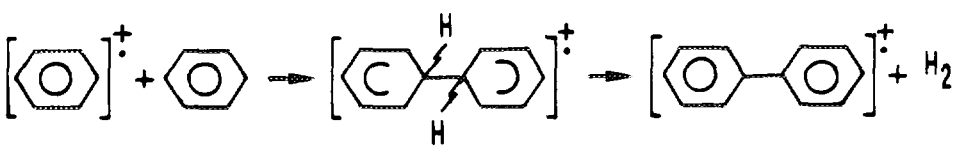

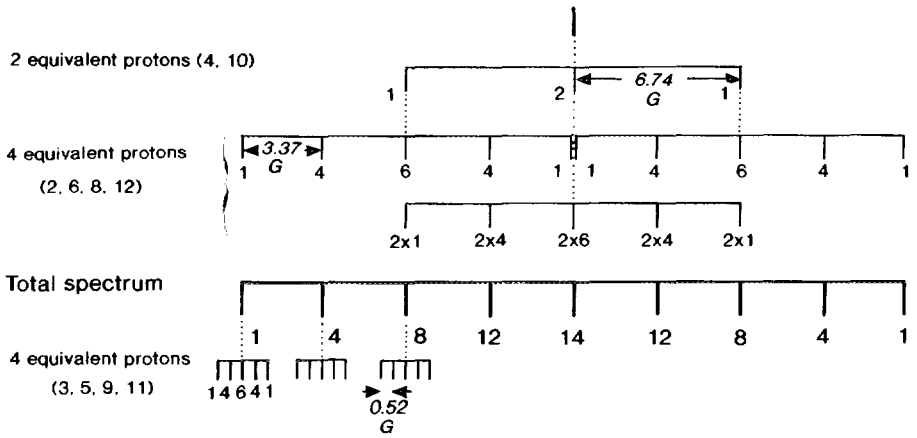

FIG. 8. Schematic representation of the hyperfine structure with the relative intensities of the biphenyl cation taking 6.74 G for protons 4 and 10 and 3.37 G for protons 2, 6, 8, and 12. The hyperfine structure due to the last four protons, 3, 5, 9, and 11, is too small and thus unresolved.

corresponding to O_2^- adsorbed on a tetravalent cation, certainly Zr^{4+}. This may presumably arise from the reaction

$$Zr^{3+} + O_2 \rightarrow Zr^{4+} + O_2^-.$$

Such a signal does not exist in the absence of benzene.

XPS analysis was performed on all samples after calcination and catalytic reaction. The main results are summarized in Fig. 11. It turns out that the S/Zr atomic ratio value was higher by about a factor two with respect to chemical analysis value. This indicates that S is not only dispersed on the surface but also in the bulk since one should expect a much higher ratio for impregnated samples (one order of magnitude more at least for a 0.1-μm crystallite size) as could be easily calculated if one considers that XPS analyses only the top 5 nm depth of the crystallites. Note also that the XPS technique showed by the binding energy values and peak shapes that on the surface S and Zr cations were mainly present in the +6

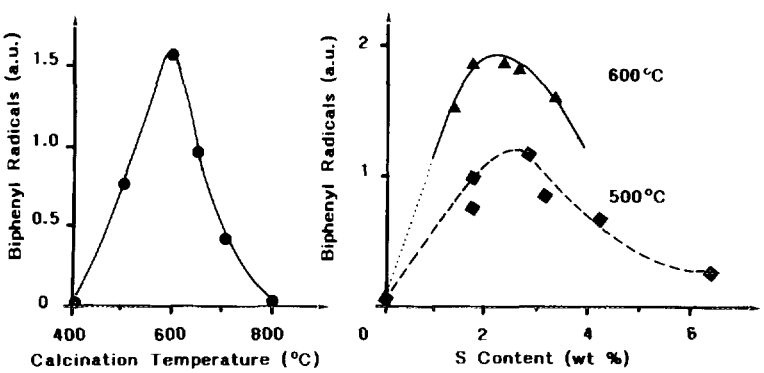

FIG. 9. Variations of ESR 9 hyperfine lines spectrum intensity (a) versus calcination temperature under static air atmosphere for the SO_4^{2-}/ZrO_2-0.08 N sample and (b) versus S content at 500 and 600°C calcination temperatures. The signal corresponds to biphenyl cations and is recorded after 5 min contact with benzene vapor at room temperature.

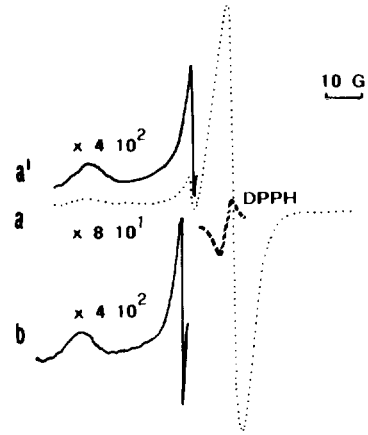

FIG. 10. RT ESR spectrum obtained after oxygen was introduced in the SO_4^{2-}/ZrO_2-0.4 *N* sample outgassed at 500°C and contacted with benzene vapor: (a) after 10 min contact with O_2 and (b) outgassed at room temperature for 30 min.

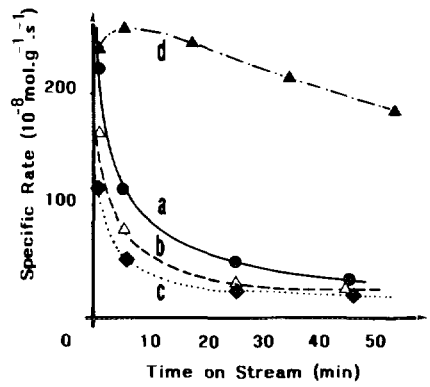

FIG. 12. Variations of the *n*-butane isomerization intrinsic rate versus time on stream at 250°C for the SO_4^{2-}/ZrO_2-0.8 *N* sample calcined at (a) 600°C, (b) 700°C, (c) 800°C, and (d) sample a in the presence of H_2.

and +4 oxidation state, respectively. Zr^{3+} cations were not detected, probably because of their low concentration. They could be identified only by ESR spectroscopy, which is a much more sensitive technique and which detects only paramagnetic species, i.e., Zr^{3+} and not Zr^{4+} cations.

These results clearly show that the active strongly acidic species are related to sulfate species. Further studies (*12*) using infrared spectroscopy and theoretical calculation are under way to describe more precisely the acid site and to bring more insight to the model proposed by Tanabe *et al.* (*3*).

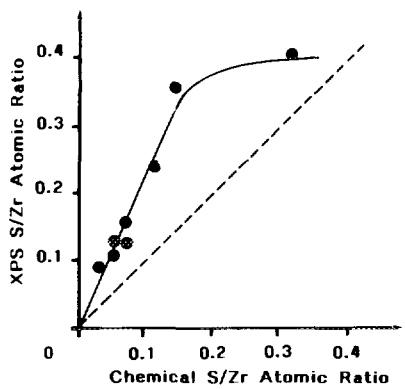

FIG. 11. S/Zr atomic ratio from XPS analysis versus chemical analysis ratio measured after calcination at 600°C and catalytic reaction. The dashed line corresponds to stoichiometric values.

Catalytic properties for *n*-butane isomerization were studied as a function of reaction temperature, precalcination temperature, and consequently of sulfur content. The main results are shown in Figs. 12 and 13 and Table 2. It is noteworthy that zirconium sulfate and samples obtained by sulfatation of zirconium oxide with the same sulfur content as those obtained starting from zirconium hydroxyde and in the same activation conditions were totally inactive.

It appears that at low temperatures and thus low conversions isomerization was the main reaction, while at higher temperatures cracking also occured with very probably a dimer (octyl) intermediate formation since propane and pentane were detected (Table 2).

The catalytic activity was observed to sharply decrease with time on stream as shown in Fig. 12, but the shapes of the curves are similar and therefore the results shown in Fig. 13 correspond to experimental values after 5 min on stream. Note that if hydrogen was used as a carrier gas, no such deactivation occured, although Pt was not

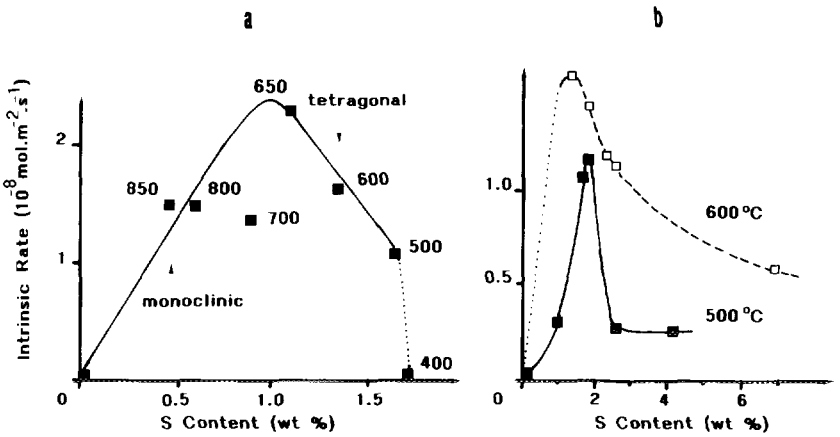

FIG. 13. Variations of the *n*-butane isomerization intrinsic rate of 250°C versus S content (a) for the SO_4^{2-}/ZrO_2-0.08 *N* at various calcination temperatures and (b) for all samples calcined at 500 and 600°C

added as it is usually the case. The same observation was recently made by Garin *et al.* (*26*).

The curves in Fig. 13 indicate that catalytic activity depends strongly on calcination temperature and on sulfur content. It is striking to observe that calcination between 400 and 500°C resulted in strong enhancement in catalytic activity while the sulfur content remained the same. This indicates that the nature of the S species is important, rather than the S content in itself.

Deactivation was observed to be very fast in the absence of Pt or H_2 and much slower in their presence. A UV–vis study of the samples after hours of time on stream was carried out for SO_4^{2-}/ZrO_2-0.08 *N* sample without H_2 in the feed and for the sample with 0.2 wt% Pt and H_2 in the feed. The spectra shown in Fig. 14 clearly show that only the highly deactivated sample exhibited an intense band near 292 nm, which may be assigned to an allylic species which presumably neutralised the active sites. Note also that without Pt but in the presence

TABLE 2

n-Butane Conversion with Flow Rate 2 dm^3 h^{-1}, P_{butane} = 9.10^3 Pa, 200 mg Catalyst, with N_2 as a Carrier Gas for the SO_4^{2-}/ZrO_2–0.08 *N* Sample

	Reaction temperature (°C)		
	200	250	300
Conversion level (%)	3	25	35
Selectivity (%)			
CH_4	—	0.4	1.2
C_2H_6	1.6	1.7	4.2
C_3H_8	0.9	2.8	13.5
i-C_4H_{10}	97.5	95.1	74.9
C_5H_{12}	0	0	6.3

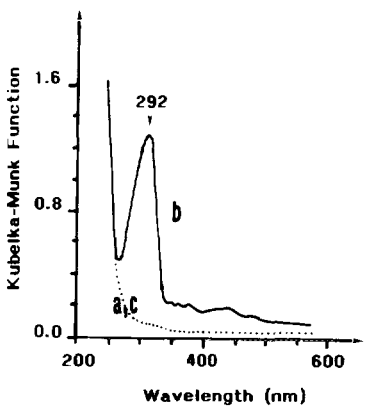

FIG. 14. UV–vis spectra of the SO_4^{2-}/ZrO_2-0.8 *N* sample (a) before reaction, (b) after reaction at 250°C for 40 min, and (c) after reaction at 250°C in the presence of 0.2 wt% Pt and hydrogen.

of H_2 the deactivation was much slower which indicates that the active species do not correspond to some reduced forms of S species since one could expect that H_2 reduced the surface more easily than butane. Moreover, XPS has shown that S is in the +6 oxidation state, and Sohn and Kim (*27*) have shown that reduction of S^{6+} species by hydrogen at 500°C decreased the catalytic activity of sulfated zirconia in the butene isomerization reaction.

It could also be possible that Brønsted acid sites were formed by action of H_2 on Lewis sites as proposed by Ebatini *et al.* (*28*) in the presence of Pt. This remains to be proved, for instance, by IR spectroscopy.

CONCLUSIONS

Several conclusions may be drawn from the above results.

Starting from freshly precipitated zirconium hydroxide, a set of SO_4^{2-}/ZrO_2 samples was prepared with a sulfur content which was observed to depend on the normality of the H_2SO_4 impregnation solutions and on the calcination temperatures.

It was observed that the formation of sites able to ionize benzene or to isomerise *n*-butane was more dependent on the calcination temperature than on the sulfur content. In particular, the samples calcined below 500°C, whatever the sulfur content was, exhibited neither catalytic nor ionizing properties. Moreover, the sulfated samples obtained from zirconium oxide rather than from zirconium hydroxide were inactive whatever the calcination temperature. Then, it is suggested that the formation of acid sites involves a two-step chemical reaction between the superficial hydroxyl groups of zirconium hydroxide and adsorbed H_2SO_4 that may be represented by the following stoichiometrical equations:

$$Zr_n(OH)_{4n} + xH_2SO_4 \leftrightarrow Zr_n(OH)_{4n-2x}(SO_4)_x + 2xH_2O,$$

and above 400°C,

$$Zr_n(OH)_{4n-2x}(SO_4)_x \rightarrow Zr_nO_{2n-x}(SO_4)_x + (2n - x)H_2O.$$

The presence of SO_4^{2-} anions in the zirconia framework may explain the sintering resistance and the stabilization of the tetragonal phase.

The existence of an optimum for the catalytic and ionizing properties as a function of the sulfur content may be due to the maximum covering of the hydroxide surface. Indeed, it is calculated that a monolayer of SO_4^{2-} anions (≈ 0.25 nm^2 per species) on a surface area equal to 100 m^2 g^{-1} represents 2 wt% S.

The nature of the sulfur species, still under study corresponds to a nonreduced sulfate-type species as evidenced by XPS (S in the +6 oxidation state) and by IR spectroscopy (*12*). Their ionizing properties are certainly related to strong Lewis-type acidity.

The limitation of the deactivation in the presence of hydrogen in the feed is certainly due, as proposed by Garin *et al.* (*25*), to a coking limitation by hydrogenating unsaturated hydrocarbons. But hydrogen could also intervene by the formation of Brønsted site, leading to a dual Brønsted/Lewis site which we propose to act as superacid site (*11*). In this hypothesis, the activation and dissociation of hydrogen should occur even in the absence of Pt, and the mechanism of formation of Brønsted sites from Lewis sites has still to be demonstrated.

REFERENCES

1. Tanabe, K., Misono, M., Ono, Y., and Hattori, N., *in* "New Solid Acids and Bases," Studies in Surface Science and Catalysis, Vol. **51**, p. 199. Kodanska, Tokyo, and Elsevier, Amsterdam, 1989.
2. Lorenzelli, V., and Tanabe, K., *in* "Advances in Acidic and Basic Solid Materials," Part I, *Mater. Chem. Phys.* **2**, 1 (1989).
3. Tanabe, K., Hattori, H., and Yamaguchi, T., *Crit. Rev. Surf. Chem.* **1**, 1 (1990).
4. Yamaguchi, T., *Appl. Catal.* **61**, 1 (1990).
5. Sijhashi, M., Hino, M., and Arata, K., *Catal. Lett.* **8**, 269 (1991).
6. Parera, J. M., *Catal. Today* **15**, 481 (1992).

7. Chen, F. R., Coudurier, G., Joly, J. F., and Védrine, J. C., *in* "Symposium on Alkylation, Aromatization, Oligomerization and Isomerization of short chain Hydrocarbons over Heterogeneous Catalysts," Preprints, ACS Petroleum Division, Vol. 36, p. 878. Am. Chem. Soc., New York, 1991.
8. Melchor, A., Garbowski, E., Mathieu, M. V., and Primet, M., *J. Chem. Soc. Faraday Trans. 1* **82,** 1893 (1986).
9. Olah, G. A., and Von Schleyer, P., "Carbonium Ions." Wiley–Interscience, New York 1968.
10. Gillespie, R. J., *Acc. Chem. Res.* **1,** 202 (1968).
11. Nascimento, P., Akratopoulou, C., Oszagyan, H., Coudurier, G., Travers, C., Joly, J. F., and Védrine, J. C., *in* "New Frontiers in Catalysis, Proceedings of the 10th International Congress on Catalysis" (L. Guczi *et al.*, Eds.), p. 1185. Elsevier, Amsterdam, 1993.
12. Babou, F., Bigot, B., Coudurier, G., Sautet, Ph., and Védrine, J. C., *in* "Acid–Base Catalysis II" (H. Hattori Ed.). Kodansha, Tokyo, 1994, in press.
13. Védrine, J. C., Auroux, A., Bolis, V., De Jaifve, P., Naccache, C., Wierzchowski, P., Derouane, E. G., B.-Nagy, J., Gilson, J. P., Van Hooff, J. H. C., Van den Berg, J. P., and Wolthuizen, J., *J. Catal.* **59,** 248 (1979).
14. Wierzchowski, P., Garbowski, E., and Védrine, J. C., *J. Chim. Phys.* **78,** 41 (1982).
15. Davis, B. H., *J. Am. Ceram. Soc.* **67,** C-168 (1984).
16. Hino, M., Kobayashi, S. and Arata, K., *Chem. Lett.*, 1027 (1988).
17. Mukaida, K., Miyoshi, T., and Satoh, T., *in* "Acid–Base Catalysis" (K. Tanabe *et al.*, Eds.), p. 363. Kodansha, Tokyo, 1989.
18. Morterra, C., Giamello, E., Orio, L., and Volante, M., *J. Phys. Chem.* **94,** 3111 (1990).
19. Lee, J. S., and Park, D. S., *J. Catal.* **120,** 46 (1989).
20. Lotkev, M. I., and Slinkin, A. A., *Russ. Chem. Rev.* **45,** 807 (1976).
21. Kurita, Y., Sonoda, T., and Sato, M., *J. Catal.* **19,** 82 (1970).
22. Nishiguchi, N., Nakai, Y., Nakamura, K., Ishizu, K., Deguchi, Y., and Takaki, H., *J. Chem. Phys.* **40,** 241 (1964).
23. Kasai, P. M., *J. Chem. Phys.* **43,** 3322 (1965).
24. Védrine, J. C., Dalmai, G., and Imelik, B., *in* "Proceedings of Colloque Ampère XV," p. 304. North-Holland, Amsterdam, 1969.
25. Che, M., and Tench, A. J., *Adv. Catal.* **32,** 1 (1983).
26. Garin, F., Andriamasinoro, D., Abdulsamad, A., and Sommer, J., *J. Catal.* **131,** 199 (1991).
27. Sohn, J. R., and Kim, H. W., *J. Mol. Catal.* **52,** 379 (1989).
28. Ebitani, K., Tsuji, J., Hattoci, H., and Kita, H., *J. Catal.* **135,** 609 (1992).